Estimation of Soil Moisture Using Optical and Fourier Transform Infra-Red Remote Sensing Techniques

By

Hafiz Syed Muhammad ZubairYounis

(2010-NUST-MS PhD-GIS-06)

A thesis submitted in partial fulfillment of the requirements for the degree of Master of Science in Remote Sensing and GIS

Institute of Geographical Information Systems
School of Civil and Environmental Engineering
National University of Sciences and Technology
Islamabad, Pakistan

August, 2014

DEDICATION

To

My Sweet and Loving Family

Thanks for understanding the stressful moments I had, for the prayers and support to overcome them and for all the joy you have brought to me.

ACADEMIC THESIS: DECLARATION OF AUTHORSHIP

I, Syed Zubair declare that this thesis and the work presented in it are my own and have been generated by me as the result of my own original research.

Estimation of Soil Moisture Using Multispectral and Fourier Transform Infrared Techniques

I confirm that:

1. This work was done wholly by me in candidature for an MS research degree at the National University of Sciences and Technology, Islamabad.
2. Wherever I have consulted the published work of others, it has been clearly attributed.
3. Wherever I have quoted from the work of others, the source has been always cited. With the exception of such quotations, this thesis is entirely my own.
4. I have acknowledged all main sources of help.
5. Where the work of thesis is based on work done by myself jointly with others, I have made clear exactly what was done by others and what I have contributed myself.
6. None of this work has been published before submission. This work is not plagiarized under the HEC plagiarism policy.

Signed: ……………………………

Date: ………………………………

ACKNOWLEDGEMENTS

Glory is to Allah, the Almighty and the Magnificent, perfect in His creations, enlightening us with the gift of knowledge and enabling us to complete our tasks successfully; Blessings upon Prophet Muhammad (peace be upon him) for guiding us towards the right path.

I owe my sincere gratitude and pleasure to my respected research supervisor Dr. Javed Iqbal, for his devoted guidance and encouraging attitude throughout the period of research, despite his multifarious preoccupations.

I am also grateful to all my guidance and examination committee members, Dr. HamzaFarooq, Dr. Nouman-ul-haq and Ms. Khunsa Fatima for their coordination and constructive criticism which directed me towards a better understanding of research and successful accomplishment of its objectives.

This research would have not been possible without the sincere cooperation and consistent support of Muhammad Tariq QAU, Islamabad. I am indebted to the entire IGIS fellows, especially Mr. Mirza Waqar, Mr. Farhan Iqbal, and Mr. Sajid Mehmood for their untiring support and assistance throughout my thesis work.

It's a pleasure to thanks all my sincere friends, colleagues and family members for their sincere attitude, support and prayers which inspired me every moment towards successful completion of my tasks.

Syed Zubair

Table of Contents

List of Figures

LIST OF NOTATIONS

Notation	Representation
º	Degrees
%	Percent
m	measured mass of the soil sample
mθ	Initial (dry) mass
ῤ w	Density of water
ῤ b	Soil bulk density
Lλ	ToA spectral radiance
ML	Band-specific multiplicative rescaling factor
AL	Band-specific additive rescaling factor
Qcal	Quantized and calibrated standard product pixel values (DN)
T	ToA brightness temperature
K1	Band-specific thermal conversion constant (B=10)
K2	Band-specific thermal conversion constant (B=11)
C	Celsius
K	Kelvin

LIST OF ABBREVIATIONS

Abbreviation	Explanation
TVDI	Temperature Vegetation Dryness Index
LST	Land Surface Temperature
NDVI	Normalized Difference Vegetation Index
FTIR	Fourier Transform Infrared Spectroscopy
NARC	National Agriculture Research Center
GPS	Global positioning system
TIR	Thermal Infrared
Ts	Surface Temperature
OLI	Operational Land Imager
LDCM	Landsat Data Continuity Mission
ETM+	Enhanced Thematic Mapper Plus
$T_s$max	Maximum Surface Temperature
$T_s$min	Minimum Surface Temperature
PARC	Pakistan Agriculture Research Center
USGS	United States Geological Survey
USDA	United States Department Of Agriculture
NIR	Near Infrared
NASA	National Aeronautics and Space Administration

ABSTRACT

Soil moisture is a key variable in hydrological process, as the availability of moisture content in soil controls the mechanism between the land surface and atmospheric processes. Accurate soil moisture estimation is decisive in weather forecast, drought monitoring, hydrological modeling, agriculture management and policy making. The objective of the study was to estimate soil moisture using remote sensed data (Fourier Transform Infra-Red spectroscopy& optical) and validation of the results with field measured soil moisture data. The ground measurements were carried out at 0-15cm depth. Combination of Normalized Difference Vegetation Index (NDVI) and Land Surface Temperature (LST) were used to derive Temperature Vegetation Dryness Index (TVDI) for assessment of surface soil moisture. Correlation and regression analysis was carried out to relate the TVDI with in-situ measured soil moisture. The spatial pattern of TVDI shows that generally low moisture distribution over study area. A significant ($p < 0.05$) negative correlation of r=0.79 was found between TVDI and in-situ soil moisture. The TVDI was also found satisfactory in temporal variation of surface moisture. The triangular method (TVDI) provides reliable estimate of moisture condition and hence can be used to assess the moisture conditions. Furthermore, the estimation of soil moisture using the triangular method (TVDI) was possible at medium spatial resolutions because the relationship of soil moisture with LST and NDVI provide significant number of representative pixels for developing a triangular scatter plot.

Chapter 1

INTRODUCTION

Soil moisture is very important biophysical parameter which is used to communicate between surface and atmosphere and also a key variable in hydrology and climate (Gao et al., 2014). It plays a vital role in understanding the hydrology, agriculture, climate, and environmental characteristics of a region (Akkuzu, Kaya, Camoglu, Mengu, & Asik, 2013). Moisture is a crucial factor enacting the budgeting of hydrological cycles especially by disuniting the rainfall into runoff, surface infiltration and evapotranspiration (Choi, Kim, & Kustas, 2011; Pollacco & Mohanty, 2012). The familiarity of soil moisture level and the processes involving the distribution of moisture are always been important in many respects. It is of importance with the arrival of agriculture in human history, information about soil moisture nowadays get important role in a much broader field, e. g. hydrology, meteorology and climatology, ecology, land surface modeling and most recently studies on global environmental changes (Willem W Verstraeten, Veroustraete, van der Sande, Grootaers, & Feyen, 2006). The issues related to environment increases, so the demand for information on environmental parameters grows synchronously. So the need for the development of more time- and cost-efficient methodologies for soil analysis is increasing. There is a wide interest for rapid and predictive soil data to be used in environmental monitoring, soil quality assessment, as well as in both precision agriculture and forestry(E. T. Engman, 1991). The system of precision agriculture, which is included among the sustainable farming systems, requires frequent environmental monitoring, including predictions of soil quality management.(Cohen M.J., 2005).

1.1 Background

Life cannot exist without water, either in a human body or a small plant. A body of human contains 85% of water and this percentage is about 90% in plants. Plants need water in transpiration, as plants lose water to atmosphere during photosynthesis. When a stomatal pore in leaves opens, water vapors transpired to the atmosphere and if sufficient quantity of water is not present in stomata pores for a particular time the leave will start wilting. Plants have to supply of water from soil to leaves through its roots to avoid wilting (Kerr et al., 2001).For this reason, water must be available in sufficient amount in soil layer from where it is to be-absorbed.

Soil water content or soil wetness is the fluid water possessing the vacant spaces between the soil particles. Water held in the 1-2 meter of soil, where it is inside the span of plant is for the most part known as accessible soil water content (Gruhier et al., 2008). Soil water content is impacted by numerous components in particular precipitation, composition and structure of the soil which decides the water holding limit of soil, slant of the area surface, which influences the overflow and invasion, vegetation, area spread which impact the evapotranspiration.

Thin soil layer may contain little amount of water as contrasted with aggregate sum of water on earth however water contained in 1-2 meter of soil controls the parceling segment of hydrological cycle (Gruhier, et al., 2008). The parceling of precipitation into surface overflow and vanishing might be dictated by examining the spatial and fleeting variability of soil water content. The variety in soil water content determinedly impacts the surface vitality parity, overflow, and evapotranspiration and vegetation benefit. The variety of soil water content in upper soil layer might be controlled by utilizing three separate sources, in-situ estimations, hydrological area surface demonstrating and remote sensing.

The ground based measurement (in-situ) is the most suitable method for determining the soil moisture's temporal variation. But in-situ measurements are not always giving precise spatial variation. At regional scale in-situ measurements are not viable, depending upon the soil properties, topography, vegetation and extrapolating them to obtain precise spatial variation is difficult (Al-Jassar & Rao, 2010; Albergel et al., 2013; Albergel et al., 2010; Benedetto & Benedetto, 2011; Bezerra et al., 2013; Brosinsky et al., 2014; Nemani, 1992).

Hydrological and land surface models are used to simulate water content at root zone. The associated uncertainty with these models become high as with same inputs and atmospheric forcing different models give different results. However researchers favor to model it as it can give an indication of spatial as well as temporal variation (Vinnikov et al., 1999), (W. W. Verstraeten, Veroustraete, & Feyen, 2005). A further disadvantage of hydrological model is the requirement of more number of inputs. A simple water balance model needs a number of meteorological and ancillary data which sometime not feasible. The high cost of ground measurements and uncertainty of hydrological and land surface models make remote sensing a feasible option.

The latest developments in technology force have made the utilization of spatial tools simple in numerous areas. The progression in remote sensing has broadened the skyline in various applications. The capacity of remote sensing to make accessible information in spatially nonstop route and over vast zone makes it a vital information hotspot for soil water content observing. Thus satellite remote sensing could be a decent interchange for the estimation of soil water content values because of its spatial scope and fleeting coherence (Blumberg, Freilikher, Kaganovskii, & Maradudin, 2002).

This thesis attempts to investigate the surface soil moisture using medium resolution satellite remote sensing data. Remote sensing methods provide tools to obtain quick estimate of soil moisture in a very cost effective mean. Remote sensing methods have the potential to obtain spatial and temporal variation of soil moisture more precisely. Optical and thermal Infrared methods proposed by (T. N. Carlson, Gillies, & Schmugge, 1995) are the best approaches for retrieving soil moisture at medium spatial resolution.

1.2 Ground Measurements of Soil Moisture

Soil samples of known weight and volume are taken for point measurements on ground. The water content is expressed as grams of water per gram of oven dry soil. Soil water contents are variable, a replication of sampling is essential for valid estimates (Ryan, Estefan, & Rashid, 2007). Soil moisture can be measured through numerous methods such as, Neutron scattering, Gamma ray attenuation, Soil electrical conductivity, tensiometer, Hygrometer, etc(Walker, Willgoose, & Kalma, 2004).The standard method for direct measurement of soil moisture is Gravimetric method. The method consists of soil samples collected from field and drying of these samples in oven at 105°C. The moisture content is then calculated by using equation 1.

$$Moisture(\%) = \frac{Wt.of soil\ (g) - Drysoil\ (g)}{Drysoil} * 100 \quad \ldots\ldots\ldots\ldots\ldots\ldots\ldots\ldots \text{Eq(1)}$$

This method is inexpensive and easy but it is time consuming. The repetitive measurements are not possible for the same location. This method is also prone to large errors due to transportation, handling of samples and repeated weighing. The measurements errors can be reduced by increasing the number and size of samples.

1.3 Soil Moisture Using Satellite remote Sensing

Remote sensing of soil moisture can be accomplished to some or all regions of electromagnetic spectrum. Estimation of soil moisture by remote sensing depends upon the reflected or emitted radiation. Soil moisture estimation through remote sensing has come long way due to its capability to monitor large area with repetitive coverage. As remote sensing is the data acquisition without being in direct contact with the object of interest using different wavelengths of electromagnetic spectrum (Campbell, 2009). The remote sensors capture the reflected or emitted signals of particular wavelengths from the earth surface. The reflected or emitted signals provide the desired information of the object of interest. Optical and microwave remote sensing has been used widely in the field of soil moisture. Optical remote sensing has used the visible and thermal infrared (TIR) spectrum.

As remote sensing has no capability of soil moisture measurement directly, mathematical models are applied to estimate the soil moisture content from the response of sensors. Forward modeling develops a set of mathematical relationships to simulate the instrument response for a given set of parameters for soil moisture these parameters generally includes soil properties, geometry and overlaying vegetation canopy (Goward, Xue, & Czajkowski, 2002).

1.4 Soil Moisture using Visible & Infrared Remote Sensing

Remote sensing of soil moisture content in near surface using visible region of electromagnetic spectrum measure the reflected radiation of the sun from the earth surface known as albedo using wavelengths(0.4-0.8 µm)(Bowers & Hanks, 1965).It has been known as having dependence upon the soil moisture status of the soil surface. There is a vast amount of literature on the use of visible–NIR and mid–IR for soil analysis(Stenberg, Viscarra Rossel, Mouazen, & Wetterlind, 2010). On the other hand this provide a poor indication of moisture content as soil reflectance is influenced by organic matters, soil texture, surface roughness, angle of incidence, plant cover and color (Goetz, Prince, & Small, 2000). Normalized Difference Vegetation Index (NDVI) developed from visible spectrum has been used broadly to monitor water stress detection and vegetation strength monitoring. As soil moisture has a direct effect on vegetation strength, there have been studies trying to relate NDVI developed from visible and infrared spectrum of remotely sensed data to the surface soil moisture. (Naira, Robert, Ramata, & Marouane, 2007) found that NDVI and soil moisture shares a linear relationship which is crop type dependent over vegetated field.

Soil moisture has different spectral patterns in different wavelengths, and remote sensing data from visible to microwave can effectively be used for its monitoring. The spectral reflectance decreases with increasing soil moisture in visible and near-infrared (NIR) range. (Zeng, 2004) developed a simple method for soil moisture monitoring by using near infrared versus red spectral reflectance space. Soil moisture monitoring by remote sensing was developed on the basis of distribution characteristics of soil moisture in the near infrared (NIR) and red spectral reflectance space. The soil moisture monitoring by remote sensing using near infrared and red was also validated with field measurements. The developed method requires only reflectance data in NIR and red wavelengths. The major limitations of optical remote sensing of soil moisture relate to surface roughness, soil structure, and the presence of organic matters.

1.5 Soil moisture Estimation using Thermal Remote Sensing

The use of remote sensing in estimating surface energy fluxes and surface soil water dates back to 1970s.It was used by geologist to locate minerals deposits (Pratt & Ellyett, 1979) and also by meteorologist to estimate the surface energy fluxes and soil water (Nemani, 1992).The information about surface energy and water status through developing the relationship between remotely sensed land surface temperature(LST) and normalized difference vegetation index(NDVI) has been investigated by many researchers(T. Carlson, 2007; E. a. C. Engman, N, 1995; Hassan, Bourque, Meng, & Cox, 2007).The correlation between thermal and visible/NIR wavelengths has proven to be useful for appropriate monitoring of vegetation and water stress. The method referred as the triangle method. The method lies on the interpretation of the pixel distribution in Ts-NDVI space. If an image contains a large range of soil water content and vegetation cover, the space presents a triangle. This triangle formed because surface temperature decreases as vegetation cover increases. The concept of triangle was first given by (Price, 1990.) and later elaborated by many researchers ((Patel, Anapashsha, Kumar, Saha, & Dadhwal, 2009),(W. W. Verstraeten, et al., 2005) while others adopted and applied the triangle method,(L. Wang & Qu, 2009),(Sandholt, Rasmussen, & Andersen, 2002).Wang et al, stated that the MODIS land parameters (LST, NDVI) are significantly correlated with ground soil moisture. They suggested that the relationships are significant enough to produce moisture estimates at moderate resolution. However, the field measurements are necessary. (Chauhan, Miller, & Ardanuy, 2003) applied this approach to obtain nearly accurate, high soil moisture by linking microwave derived soil moisture with optical parameters.

1.6 Fourier Transform Infra-Red Spectroscopy

Fourier Transform Infra-Red spectroscopy is mostly used technique of infrared spectroscopy. When infrared radiations passed from a sample, some of it is absorbed by the sample and the remaining passed through. The spectrum formed represents patterns of absorption and transmission, forming molecular values of the sample. Every structure produces different line spectrum. This makes infrared spectroscopy useful for several types of analysis. An important aim of sustainable agriculture is to maintain a certain quality of the soil, and thus soil fertility. One way to assess the soil quality, or some of the qualitative parameters of the soil, is by the use of non-destructive FTIR spectroscopy. FTIR spectroscopy was used successfully on whole soils to describe the status of decomposition within the different horizons (Haberhauer & Gerzabek, 1999).

Water in itself is essential for plant growth and its presence in the soil influences numerous properties such as the availability of oxygen and nutrients, microbial activity, swelling and shrinking of clays or soil stability. Since the methods traditionally used to estimate water related soil properties are time consuming, much research has been devoted to the development of alternative methods. In particular, very good results have been reported for some of these properties using near-infrared spectroscopy under laboratory conditions(Mouazen, Karoui, De Baerdemaeker, & Ramon, 2006),(Viscarra Rossel & McBratney, 1998)and encouraging results have been reported for in-situ field measurements. The need for fast and cheap methods that would enable the analysis of a large number of samples has been stressed in numerous studies (Viscarra Rossel & McBratney, 1998)and infrared spectroscopy has long been recognized as one of the most promising techniques. As in other applications, the initial works were conducted mainly in the near-infrared (NIR) range for which instruments were readily available. Technological achievements in the mid-infrared (mid-IR) range during the last decade have made this spectral range much more attractive and an increasing number of soil studies are conducted using this spectral range.

1.7 Rationale

Studying the spatial and temporal variations of soil moisture at regional level is important in hydrological application, river flow forecasting, irrigation management, soil conversations measurements, agriculture development, meteorology etc. The applications range from weather and climate predictions for early warning of flood, drought and socioeconomic activities like agriculture, water management and policy making. The information about soil moisture is also important for crops. Crop productivity is damagingly affected if crop is not supplied with ample soil moisture. The monitoring of soil moisture provides better crop production information than rainfall or weather forecast and helps farmers in decision making.

The decrease in soil moisture leads to decline in crop yield, which result in agriculture drought. Agriculture plays vital role in people's day to day life as well as country economy, so recurring drought put a great threat to sustainable development. Soil moisture information can help in early detection of drought and evaluation of drought impact on agriculture.

There is frequent need of measurements for describing the soil moisture behavior. The advance apparatus measure soil moisture and describe temporal variability only at specified location. The spatial and temporal variability of soil moisture over large extent is difficult to measure using such advance equipment. The interpolation between conventional point base methods do not yield precise results because the method do not consider the surface roughness, vegetation condition, topography and other precursor condition. The cost of in-situ measurements and data demands to think about a free data source (remote sensing). This is main reason to explore other techniques such as remote sensing to infer surface soil moisture status and information of its spatial and temporal distribution(Nemani, 1992). Soil moisture is commonly assessed by point based method (gravimetric method) in fields, but this method is time consuming and do not describe behavior of its spatial and temporal distribution. Also the in situ measurement techniques of soil moisture in general are tedious and not performed on routine basis.

Modern technological advancement has shown that soil moisture can be estimated by variety of remote sensing techniques. Especially the techniques in optical/IR and microwave have engrossed more attention (Vinnikov, et al., 1999),(W. W. Verstraeten, et al., 2005).The channel frequency and spatial resolution of microwave radiometer are not optimal for land remote sensing due to practical problem in supporting a large low frequency antenna in space(Blumberg, et al., 2002).

Hence the confront task was to use the novel optical/IR approach based on triangular method proposed by (Sandholt, et al., 2002).Landsat data appears to be fine for monitoring the soil moisture over the area with large coverage. There are several methodologies for estimation of soil moisture using remote sensing, including thermal inertia approach, crop water stress index method, normalized vegetation index scheme, crop water deficit index method. The temperature vegetation dryness index (TVDI) derived from satellite data is used to monitor soil moisture (Sandholt, et al., 2002). In the last decade, a number of researchers have analyzed the relation between and surface temperature (Ts) and vegetation indices (NDVI).

(Moran, Clarke, Inoue, & Vidal, 1994)described a method based on the Ts/NDVI trapezoid. The TVDI is calculated based on the interpretation of relationship between vegetation indices (NDVI) and LST (TS) (Atchley & Maxwell, 2011;

dall'Amico et al., 2013; Fan & van den Dool, 2011; Fang et al., 2013a, 2013b; Guo, Yang, & Wang, 2011; Hejazi & Woodbury, 2011; Holzman, Rivas, & Piccolo, 2014; Liu, Liu, Wang, & Zhu, 2012; Lopes et al., 2011; Mei & Wang, 2011; Parinussa, Holmes, Yilmaz, & Crow, 2011; Pause, Schulz, Zacharias, & Lausch, 2012; Ridler et al., 2012; C. Y. Song, Jia, & Menenti, 2014; X. N. Song, Leng, Li, Li, & Ma, 2013; Srivastava, Han, Ramirez, & Islam, 2013; Sun, Sun, Li, Liang, & Zhang, 2012; Tennant & Beare, 2014; A. Q. Wang, Xie, Shi, & Gong, 2013; W. Wang, Huang, Wang, Liu, & Zhou, 2011; Wu, Jansson, & Zhang, 2011; Zhao & Li, 2013; Zhao et al., 2013). In present study soil moisture was estimated by linking the temperature vegetation dryness index (TVDI) with ground observation & FTIR technique using Land sat 8 data.

1.8 Objectives

The objectives of the study were to (1) estimate soil moisture using remote sensed data (FTIR& optical) and field measured soil moisture (2) validate remotely sensed soil moisture data with soil data measured in laboratory.

Chapter 2

MATERIALS AND METHODS

2.1 Study area

The study area (latitude 33º. 43´ N, longitude 73º 04´ E, with altitude 490 msl) selected was National Agricultural Research Centre (NARC), Islamabad (Fig. 1). The total area of NARC is approximately 566 hectares and located near Rawal Lake, six kilometers south-east of Islamabad. Physical facilities in term of experimental fields, laboratories, green houses, gene bank, library, documentation, auditorium, machinery and lab equipment repair workshops, stores, hostels, cafeteria, audio visual studios, are also available at NARC.

2.1.1 Climate of the study area

The study area has a typical version of humid subtropical climate, covering the entire major five seasons: Winter (Nov−Feb), spring (March−April), summer (May−June), Rainy Monsoon (July−August) and autumn (September−October). The hottest month is June, where average highs routinely exceed 38 °C (100.4 °F) (Fig. 2). The wettest month is July, with high rainfall and thunderstorms. The coolest month is January, with temperatures variable by location. In Islamabad, temperatures vary from cold to mild, routinely dropping below zero. In the hills there is sparse snowfall. The average low temperature is 2 °C (35.6 °F) in January, while the average high temperature is 38.1 °C (100.6 °F) in June (Fig. 3).

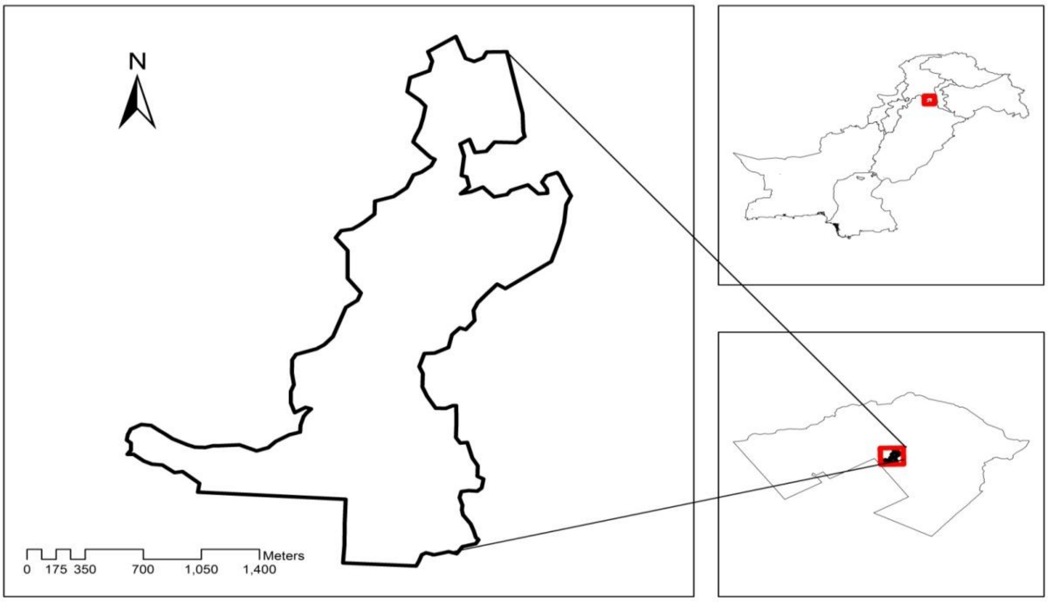

Figure 1. Study area NARC Islamabad.

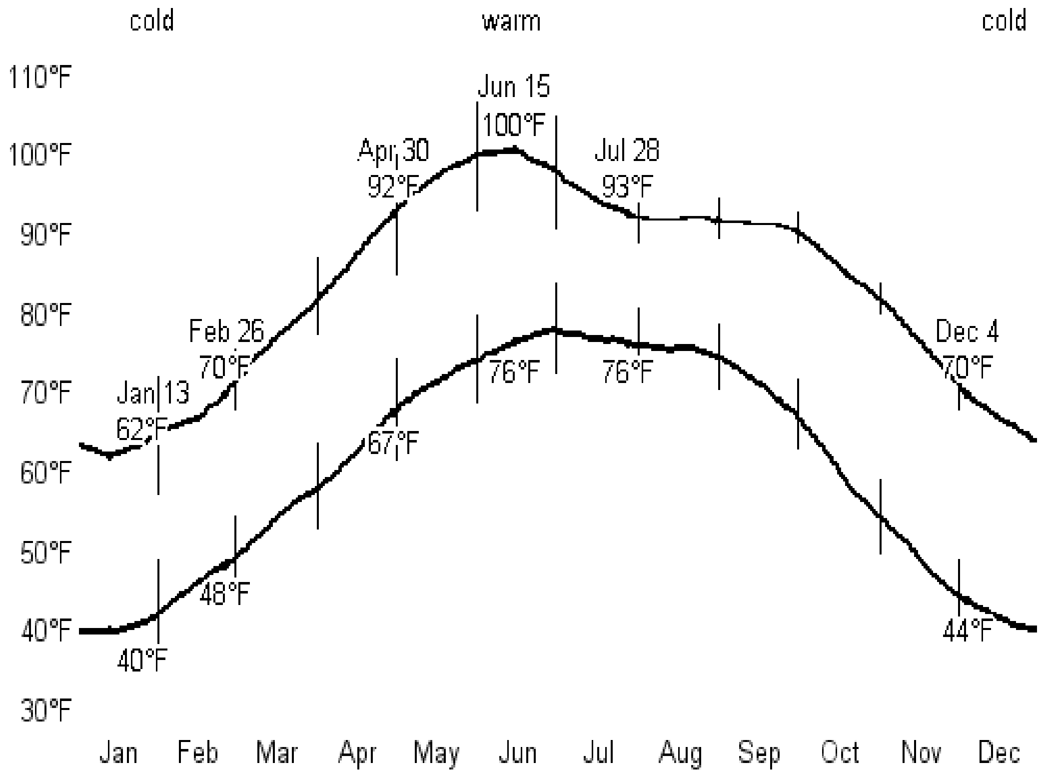

Figure 2. Climate of study area.

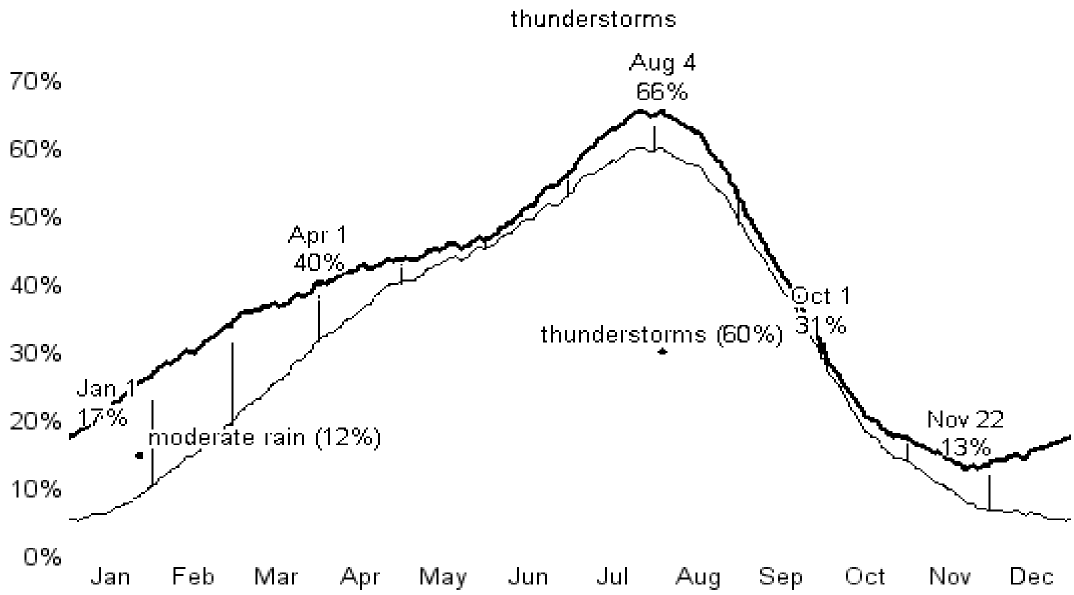

Figure 3. Rainfall pattern of study area.

2.1.2 Soils of the study area

A soil is three dimensional conceptual unit in which numerous physical, chemical and biological processes takes place. It is a thin layer of material on the Earth surface in which plants have roots. Changes in different kind of energy derived these processes. A fraction of solar energy is transformed into heat energy which results in increase in soil temperature of surface soil. This results in high evaporation of water in soil particles. The site was a Nabipur soil series, classified as Typic Camborthid (Calcaric Fluvisols). The soil is developed from a mixed, calcareous alluvium, and is weakly differentiated, they are generally medium textured to clay-loam with native organic matter as low as <2.5g kg-1. The soil moisture pattern of the study area follows the rainfall pattern. In dry season the soil moisture content are low and during the rainy season the moisture content increases. The study area consists of 4 soil types namely silt clay, clay loam, loam, silt clay loam.

2.1.3 Land Cover of study area

The agriculture land of the study area is very fertile. As NARC is a research center number of crops have been grown there for research purposes the major crops are cereals legumes vegetables fruits etc.

2.2 Methodology

The study attempts to measure soil moisture using medium resolution optical remote sensing satellite data. In situ measurements were also carried out during field visit of the study area. This chapter explains the data used to attain the objective and methodology adopted for study.

2.3 Field Work

The field work was performed in March 2013 to collect the primary soil moisture data. The main activity during the field was to measure soil moisture using direct method.

For this purpose 120 soil samples were collected from the whole study area by using soil auger. Randomized sampling was done to cover the study area (Fig. 4). GPS points of each sample was recorded at the time of sampling Samples were placed in sealed polythene bags and transferred to soil laboratory for moisture & texture analysis.

2.4 Soil Moisture Measurement Using Gravimetric Method

Soil samples were collected randomly from the study area from 0-15 cm depth. Samples were dried, crushed, sieved and finally bagged for further lab analysis (Fig. 5). In the lab for analysis of gravimetric soil moisture content a 50 gm sample was placed in oven at 105°C for 24 hrs. The dried soil samples were weighed using a Mettler Balance and the percent gravimetric soil moisture was calculated (Equation 2):

$$\text{Moisture}(\%) = \frac{\text{Wt.ofsoil (g)} - \text{Drysoil (g)}}{\text{Drysoil}} * 100 \quad \ldots\ldots\ldots\ldots\ldots\ldots\ldots\ldots\ldots\ldots\ldots\ldots\ldots$$

Eq. 2

2.5 Soil Texture Analysis

Texture, or size distribution of mineral particles (or its associated pore volume), is one of the most important measures of a soil because finely divided soil particles have much greater surface area per unit mass or volume than do coarse particles. Thus, a small amount of fine clay and silt will be much more important in chemical reactions, release of nutrient elements, retention of soil moisture, etc., than a large volume of coarse gravel or sand.

Soil (mineral) particles are broadly segregated into three size classes (1) sand - individual particles visible with the naked eye, (2) silt - visible with a light-microscope, and (3) clay - some may not be visible with a light-microscope, especially the colloidal size (i.e., < 1 micrometer or 0.001 millimeter). The sand, silt and clay groups are commonly referred to as the soil separates; soil texture is defined as the relative proportions of each class. Soil content of fine particle sizes is so important in determining the fertility and water-supplying capacity as well as tillage characteristics of soils that it is used as one of the primary descriptive characteristics for classifying soil horizons and soil profiles. The U.S. Department of Agriculture (USDA) soil textural classes are shown on the soil texture triangle (Fig. 6).

2.6 FTIR Spectroscopy Analysis

The FTIR spectroscopy analysis was carried out at Quaid-e-Azam University Islamabad chemistry department. Composite of soil samples were made on the basis of texture classes. Five composite samples for each texture class were taken for FTIR analysis. The wavelength spectrum has variations on different soil moisture conditions which can be seen during FTIR analysis on soil samples, as moisture increases the soil reflectance decreases (Lobell & Asner, 2002) this method can be helpful for satellite remote sensing of soil moisture.

Reflectance measurements were acquired in a laboratory by using a full-range (500–2500 nm) spectrometer. After measuring the reflectance of the oven-dried sample, de-ionized water was applied to the soil with a pipette until the soil was deemed near saturation. Spectral measurements were then collected repeatedly until the soil mass returned to its initial value (after 1 h). Water content was determined from mass measurements recorded throughout the experiment, and expressed on a volumetric basis. Moisture content was calculated for each spectral measurement from equation 3:

$$\frac{m - m\theta \,/\, \rho w}{m\theta \,/\, \rho b} \times 100 \quad \text{.................................Eq.3}$$

Where:

m= measured mass of the soil sample.
mθ = initial (dry) mass.
ρ_{w} = density of water (1.0 g/cm^3).
ρ_{b} = soil bulk density.

2.7 Remote Sensing Data Acquisition

Landsat 8 (OLI & TIRS) data was acquired to estimate the soil moisture content of surface layer. The imagery was cloud free and downloaded from United States Geological Survey (USGS) website the particulars of data acquired were, WRS_PATH = 150 WRS_ROW = 37.

2.8 Landsat 8 Sensor

Landsat 8 is an American Earth observation satellite launched on February 11, 2013. It is the eighth satellite in the Landsat program; the seventh to reach orbit successfully. Originally called the Landsat Data Continuity Mission (LDCM), it is collaboration between NASA and the United States Geological Survey (USGS).

NASA Goddard Space Flight Center provided development, mission systems engineering, and acquisition of the launch vehicle while the USGS provided for development of the ground systems and will conduct on-going mission operations.

The Landsat 8 program, jointly managed by NASA and the USGS, provides satellite data that is in the public domain and free. The satellite orbits Earth every 99 minutes at an altitude of 705 kilometers (438 miles) in a polar orbit. The satellite records the daylight side of Earth on the soutbound leg of its orbit. It collects about 400 new scenes comprising 400 GB of data every day. Processed data becomes available to the public within 24 hours of collection. Despite voluminous data collection, it will take several years before cloud-free scenes are available for most areas. Obtaining cloud-free images of some very wet tropical areas may never happen. Regular coverage includes the area between 82° 40' north and south latitude. Off-nadir (sideways looking) scenes extend coverage to slightly higher latitudes, but not as far as the poles. The satellite returns to the same place on Earth occur every 16 days and at the same time of day. It records new scenes depending on the weather below and other collection requirements. The mid morning hours are when the satellite records scenes everywhere on Earth. It crosses the equator at around 10:00 AM. Scenes are north-oriented. However, because Earth rotates east as the southbound satellite flies over it; the area covered in scenes follows the northeast to southwest trending flight paths. Along flight path axes, Landsat 8 scenes measure 185 kilometers wide by 170 kilometers tall (115 x 105 miles). The scenes are georeferenced and orthorectified to elevation data. They are in the UTM/WGS 84 coordinate system. Downloaded bands come as 16-bit grayscale geotiffs, which are ordinary .tiff images, but with extra georeferencing information. Note that the satellite sensors collect raw data at the 12-bit depth. Interpolation accounts for the greater bit-depth of the released data. The ground resolution (how much distance each pixel represents on Earth) of the bands is generally 30 meters. Band 8 containing panchromatic data at 15-meter resolution is an important exception. Bands 10 and 11 are up-sampled to 30-meter resolution from data collected at 100-meter resolution (Patterson, 2013).

2.9 Operational Land Imager

Landsat 8's Operational Land Imager (OLI) improves on past Landsat sensors and was built, under contract to NASA, by Ball Aerospace. OLI uses a technological approach demonstrated by the Advanced Land Imager sensor flown on NASA's experimental EO-1 satellite. The OLI instrument uses a pushbroom sensor instead of whiskbroom sensors that were utilized on earlier Landsat satellites. The pushbroom sensor aligns the imaging detector arrays along Landsat 8's focal plane allowing it to view across the entire swath, 115 miles (185 kilometers) cross-track field of view, as opposed to sweeping across the field of view. With over 7,000 detectors per spectral band, the pushbroom design results in increased sensitivity, fewer moving parts, and improved land surface information. OLI collects data from nine spectral bands. Seven of the nine bands are consistent with the Thematic Mapper (TM) and Enhanced Thematic Mapper Plus (ETM+) sensors found on earlier Landsat satellites, providing for compatibility with the historical Landsat data, while also improving measurement capabilities. Two new spectral bands, a deep blue coastal / aerosol band and a shortwave-infrared cirrus band will be collected, allowing scientists to measure water quality and improve detection of high, thin clouds.

2.10 Thermal Infrared Sensor

The Thermal Infrared Sensor (TIRS), built by the NASA Goddard Space Flight Center, conducts thermal imaging and supports emerging applications such as evapotranspiration rate measurements for water management. The TIRS focal plane uses GaAs Quantum Well Infrared Photo detector arrays (known as QWIPs) for detecting the infrared radiation—a first for the Landsat program. The TIRS data will be registered to OLI data to create radio-metrically, geometrically, and terrain-corrected 12-bit Landsat 8 data products. Like OLI, TIRS employs a pushbroom sensor design in addition to a 185 kilometer cross-track field of view. Data for two long wavelength infrared bands will be collected with TIRS; however, TIRS only provides Landsat data continuity with one band—Band 10. With TIRS being a late addition to the Landsat 8 satellite, the design life requirement was relaxed in order to expedite development of the sensor. As such, TIRS only has a three-year design life.

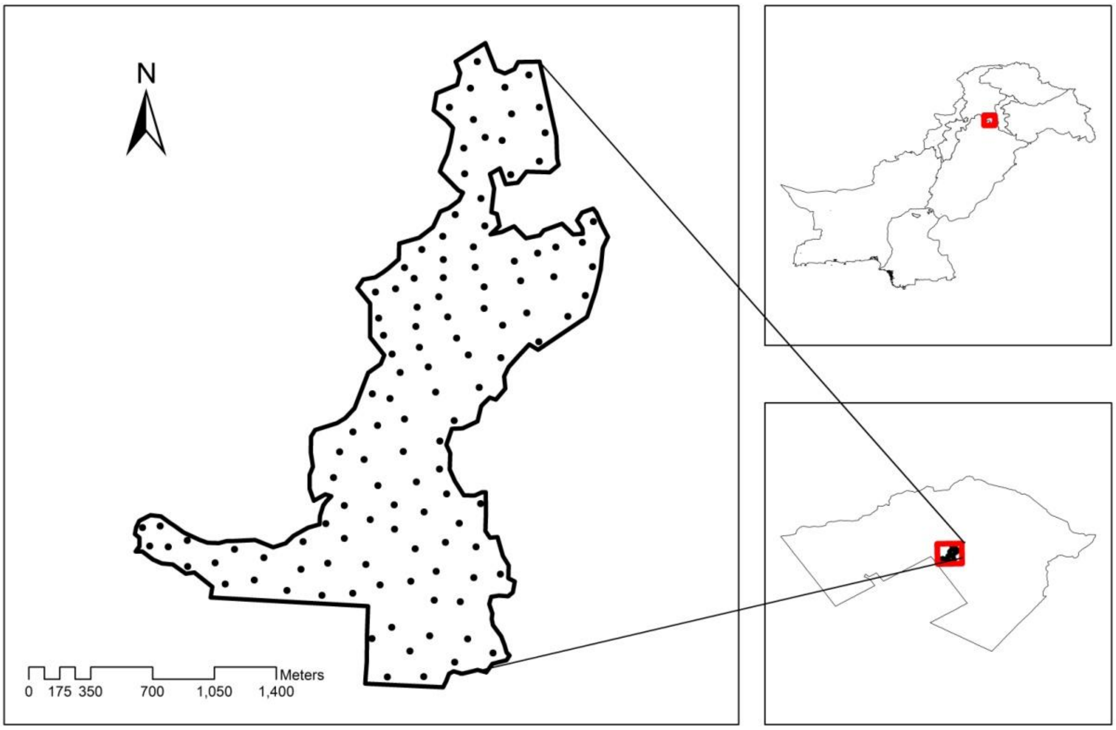

Figure 4. Sample points distribution over study area.

Figure 5. (a) Field sampling carried out by using soil auger (b) GPS points were taken for each sample (c) packing of soil samples in polythene bags (d) samples ready for lab analysis.

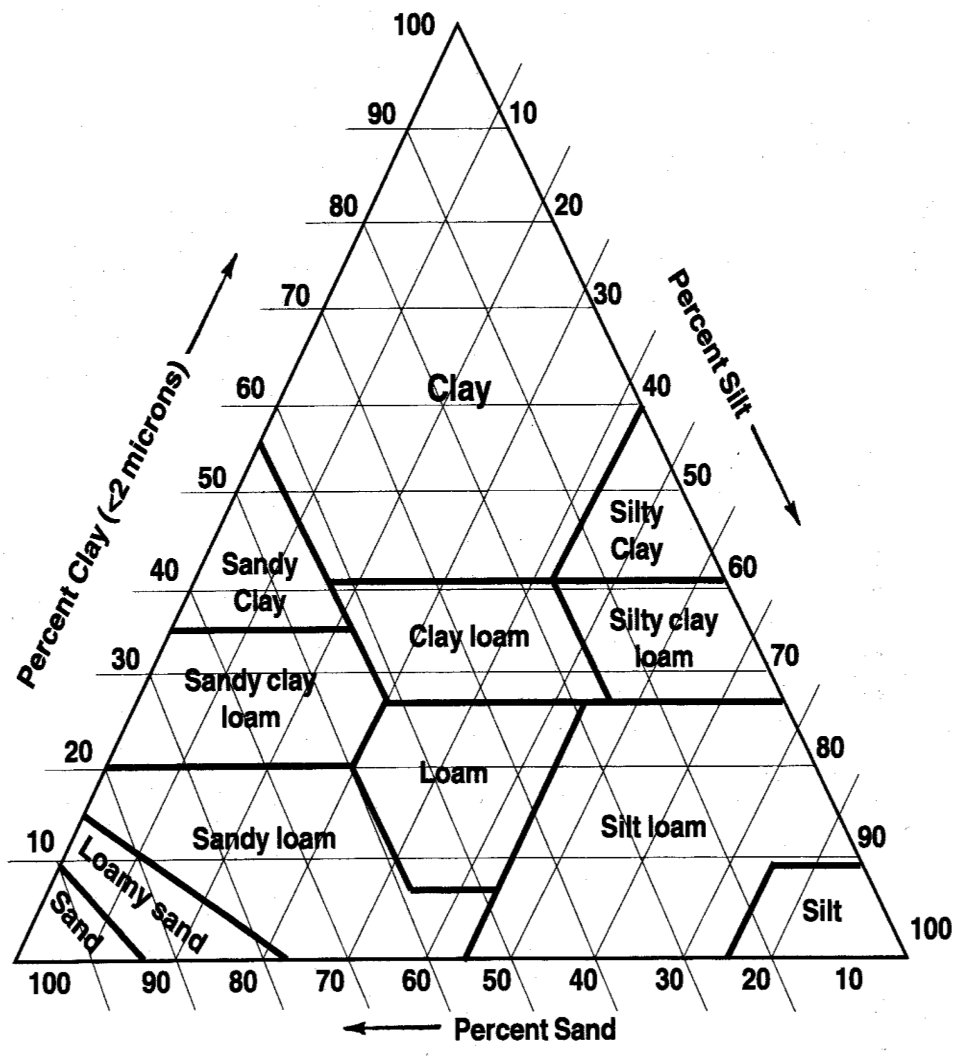

Figure 6. USDA Soil Texture Triangle.

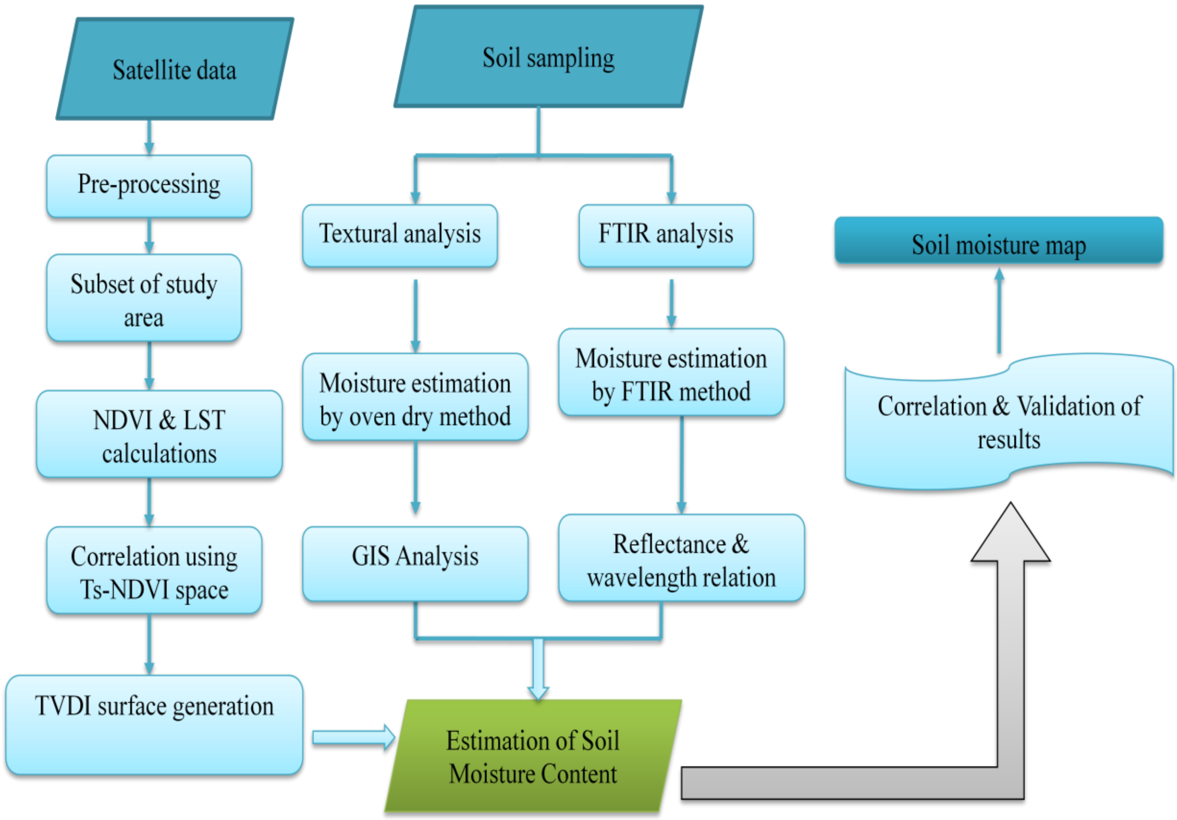

Figure 7. Detailed flow chart methodology of the research study.

Chapter 3

RESULTS AND DISCUSSION

3.1 Soil Moisture lab Analysis

The conventional method was carried out to determine the soil moisture conditions of the study area. The results shows variability of 2-10% of soil moisture of all samples distributed over study area (appendix-1).

3.2 Soil Texture Analysis

The most common method used for soil texture determination involves soil texture triangle to distinguish the textural classes. The classification depends on the amount of percent silt, sand and clay in a given sample. Soil texture plays important role in retention of soil moisture as clay soils have more water holding capacity than silt and sand. The results shown 4 texture classes i.e. silt clay, clay loam, silt clay loam and loam.

3.3 FTIR Analysis

FTIR is a technique which is used to determine the reflectance in a given sample. In this method samples were placed under a full range spectrometer (500-2500nm). Soil samples were arranged on the basis of texture classes and 5 composite samples were taken from each texture class which was representative of whole study area.

The study quantify changes in soil reflectance as a soil proceeded from wet to dry states and to determine the dependence of these changes on soil type and wavelength. This will develop a quantitative relationship between soil moisture and reflectance that minimized differences between soil types for use in operational soil moisture retrieval algorithms and canopy radiative transfer models.

Reflectance decreases with increasing moisture for all soils (Fig. 8) below except there was a certain region of SWIR where the behavior of curve went higher because of absorption region for water molecules(Muller & Decamps, 2001).

3.4 Remote Sensing of Soil Moisture

For remote sensing approach Landsat-8 imagery was used whose general introduction is already mentioned. To estimate surface soil moisture triangulation method was used which is a common method to estimate soil moisture. This method is a combination of visible, infrared and thermal datasets. The information about surface energy and water status through developing the relationship between remotely sensed land surface temperature (LST) and Normalized difference vegetation index (NDVI) has been investigated by many researchers. Correlation between thermal and visible/NIR wavelengths has proven to be useful for appropriate monitoring of vegetation and water stress. The method lies on the interpretation of the pixel distribution in Ts-NDVI space. If an image contains a large range of soil water content and vegetation cover, the space presents a triangle. Triangle formed because surface temperature decreases as vegetation cover increases. Scatter plot between NDVI & LST is called the Ts-NDVI space and closely related to surface evapotranspiration and surface moisture etc (Fig. 9).The method of mapping soil moisture using LST and NDVI is called TVDI.

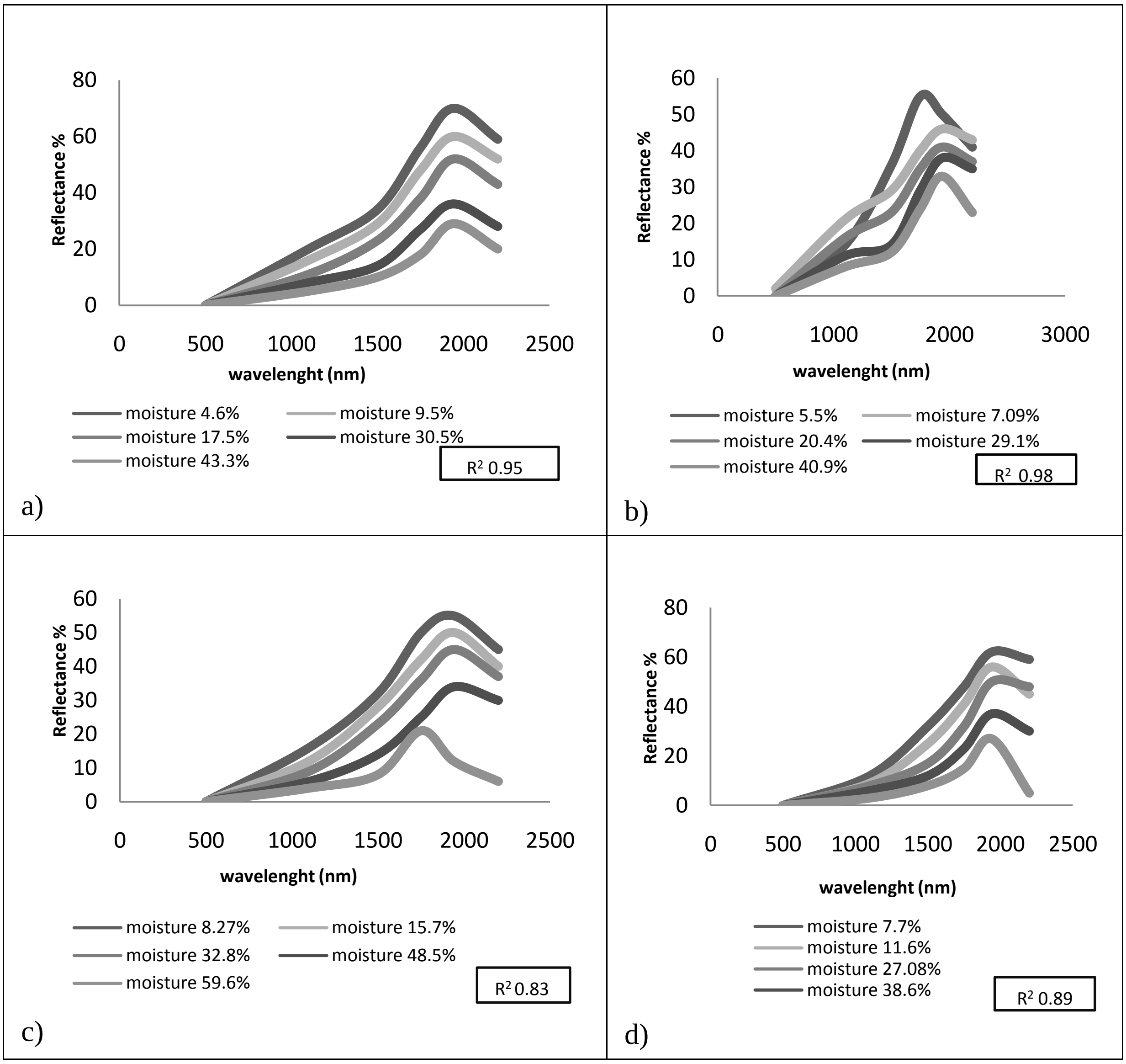

Figure 8. Relationship of soil moisture and reflectance (a) silt clay loam (b) loam (c) clay loam (d) silt clay.

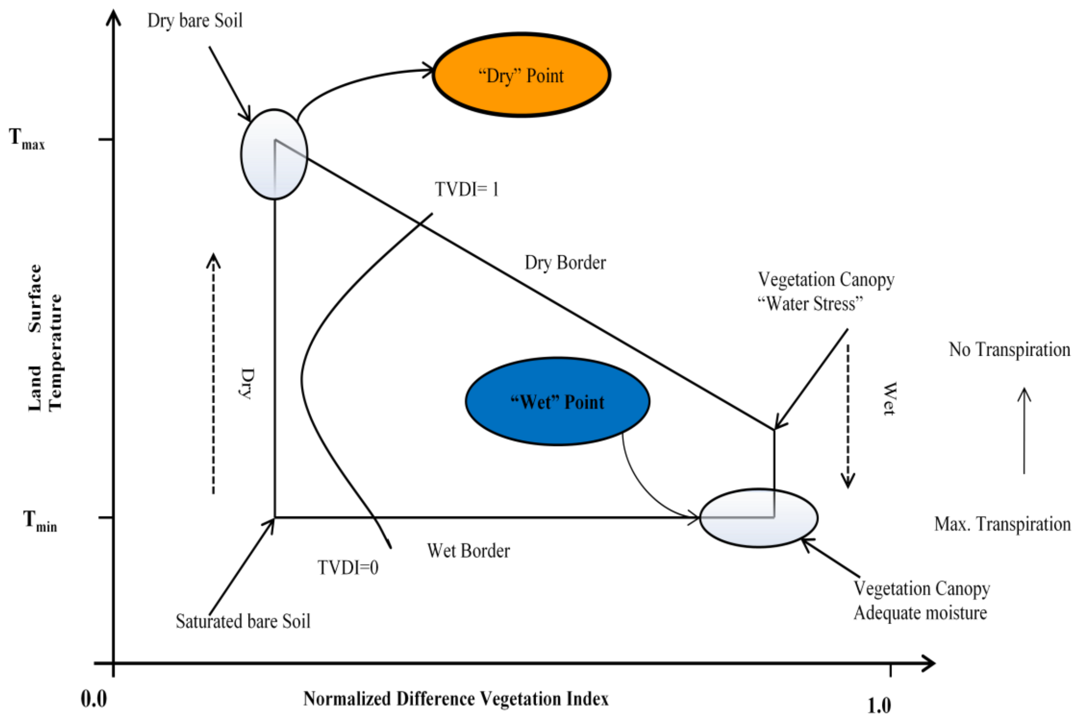

Figure 9. Surface temperature and normalized difference vegetation index scatter plot.

3.5 Normalized Difference Vegetation Index

Vegetation indices are based on reflection characteristics of plant leaves in visible (VIS) and near-infrared (NIR) portion of light. Healthy vegetation has low reflectance of visible light (0.4-0.7µm) as it is strongly absorbed by the leaf stain for photosynthesis. High reflectance is observed in near-infrared light (0.7-1.1µm) for healthy vegetation. NDVI can be calculated by the ratio between visible and near-infrared bands of satellite image. Mathematically equation 4 can be written as follow,

$$NDVI = \frac{Ref\,(NIR) - Ref\,(Red)}{Ref\,(NIR) + Ref\,(Red)} \quad \text{……………………………………………Eq.4}$$

The formula was applied by using Erdas Imagine model builder. NDVI values are always lie between -1 and 1.Higher values represents the healthy status of vegetation. Lower values (0.1 and low) represent the bare area of rocks, sand and snow. Moderate values (0.2-0.3) correspond to shrub and grassland. Temperate and Tropical rainforest are represented by high NDVI values (0.6-0.8).NDVI is an indicator and assessment of live green vegetation using satellite imagery. It is an equation that takes into account the amount of infrared reflected by plants. Live green plants absorb solar radiation, which they use as a source of energy in the process of photosynthesis. The reason NDVI is related to vegetation is that healthy vegetation reflects very well in the near-infrared part of the electromagnetic spectrum. The value of NDVI ranges from 0.02 to 0.54 of study area. The map of NDVI has shown in Fig. 10.

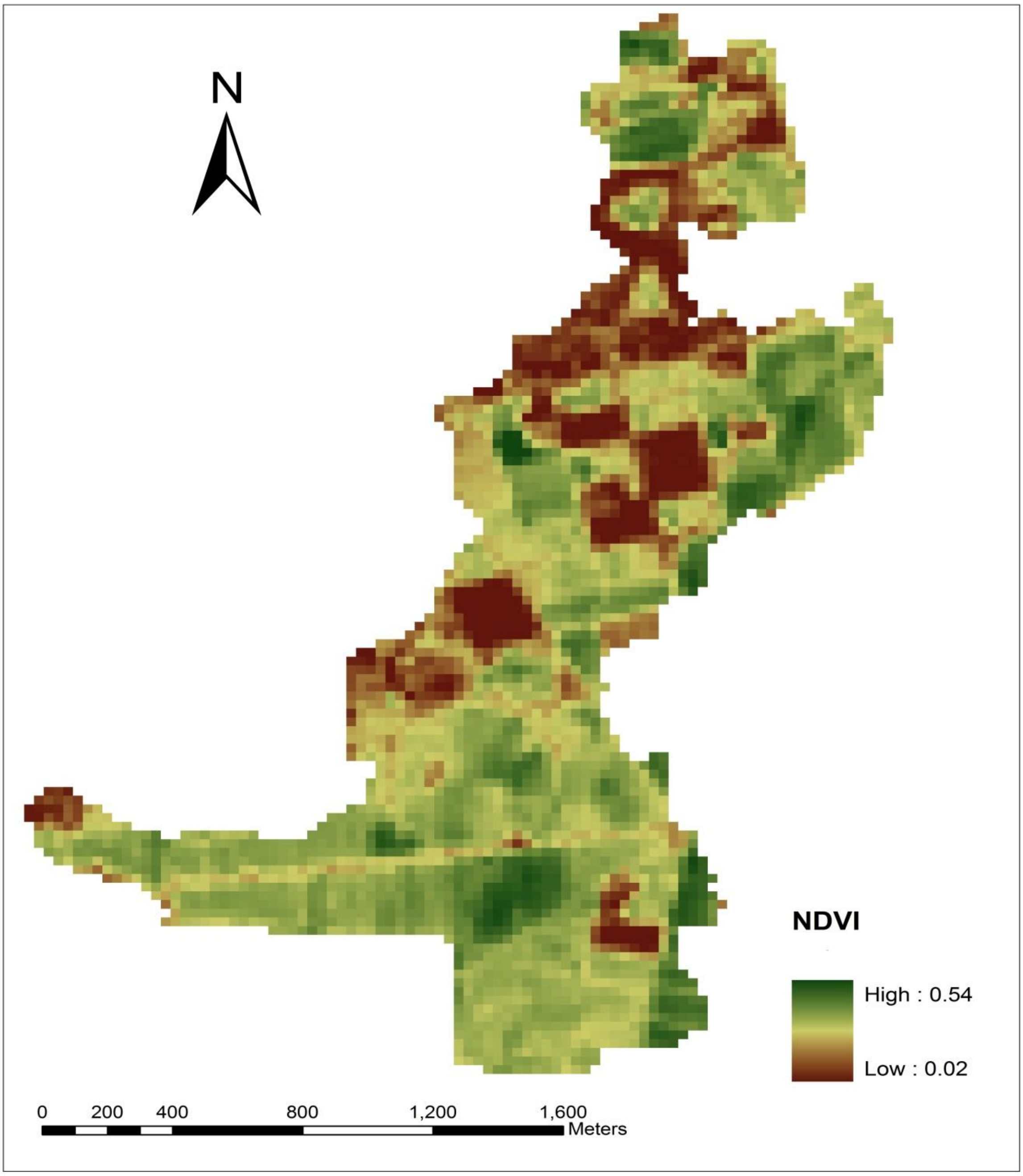

Figure 10. Normalized difference vegetation index of study area.

3.6 Land Surface Temperature

Land surface temperature is also the surface atmosphere interaction and energy fluxes between ground and the atmosphere on earth including thermal emission from landscape surface which includes top of the canopy for vegetated surfaces as well as the other surfaces such as bare soil. Surface temperature was calculated from satellite image's thermal band. In Landsat 8 there are 2 thermal bands the brightness of both bands were calculated and then the average was taken as LST of the study area. To obtain actual surface temperature information, first convert the DNs to top-of-the-atmosphere (ToA) radiance values, and then secondly convert the ToA radiance values to ToA brightness temperature in Kelvin. The equation 5 was used to convert Digital Numbers into ToA radiance values.

$L\lambda = (ML * Qcal) + AL$…………………………………….. Eq.5

Where:

L_{λ} = ToA spectral radiance

M_L = Band-specific multiplicative rescaling factor

A_L = Band-specific additive rescaling factor

Q_{cal}= Quantized and calibrated standard product pixel values (DN)

After getting the radiance values these were converted into temperature brightness by using the following (Equation 6):

$T = K2 / (ln (K1/ L\lambda + 1))$.. Eq.6

Where:

T = brightness temperature (K)
L_{λ} = spectral radiance
K_1 = Band-specific thermal conversion constant
K_2 = Band-specific thermal conversion constant

The temperature values result in Kelvin which then converted into degree Celsius by applying simple equation (C = K-273). The temperature values of LST ranges from 33.19 to 40.57. Map was created by using arcgis which shows the variation in temperature among the study area (Fig. 11).

3.7 Temperature Vegetation Dryness Index

TVDI was calculated by using the values of LST and NDVI. The values of both were rounded to two decimals and exported to dbf files. They were plotted against each other in excel sheet to identify the regression lines defining the upper and lower edges of triangle. The Ts-NDVI space was created to identify the dry and wet edges of the area. The procedure was applied to the image and wet and dry edges were identified by the pixel distribution of LST and NDVI (Sandholt et al. 2002) analyzed the triangle formed by the scatter plot of two parameters LST and NDVI representing Ts-NDVI space and used this space for the definition of TVDI. After this the TVDI can be calculated by using the equation 7:

$$\text{TVDI} = \frac{\text{Ts} - \text{Tsmin}}{\text{Tsmax} - \text{Tsmin}} \quad \text{...Eq.7}$$

Where:

Ts= land surface temperature of any pixel.
Tsmin= minimum land surface temperature.
Tsmax= maximum land surface temperature.

There was a strong correlation found between LST and NDVI. In (Fig. 12) y-axis represents the land surface temperature and x-axis shows normalized difference vegetation index. The relationship between LST and NDVI shows decreasing temperature with increasing vegetation and increasing temperature with decreasing vegetation. After getting the dry and wet edges the values were exported in arcgis to draw TVDI map. The TVDI values ranges from 0 to 1(Fig. 13).

3.8 Validation of results

After getting the TVDI surface it was compared by physically measured soil moisture. The values of satellite measured soil moisture in the form of TVDI were exported to dbf format to perform correlation analysis. The result shows that as the TVDI value decreases the physically measured moisture increases and vice versa (Fig. 14). So this was derived that there was a moderately strong correlation between TVDI and actual soil moisture. The RMS value recorded was 0.79.The final map of soil moisture of the study area shown in Fig. 15.

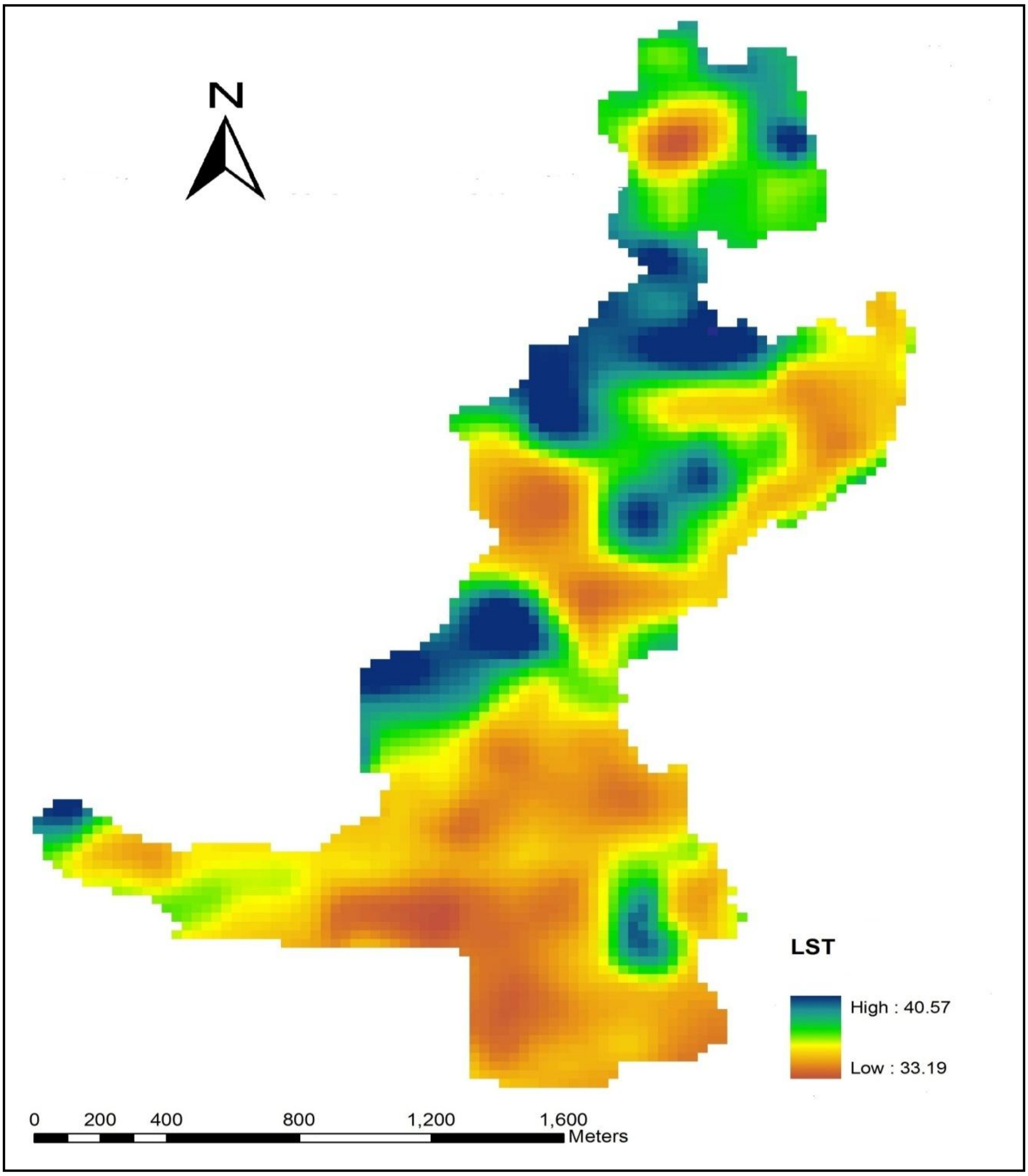

Figure 11. Land surface temperature of study area. (°C)

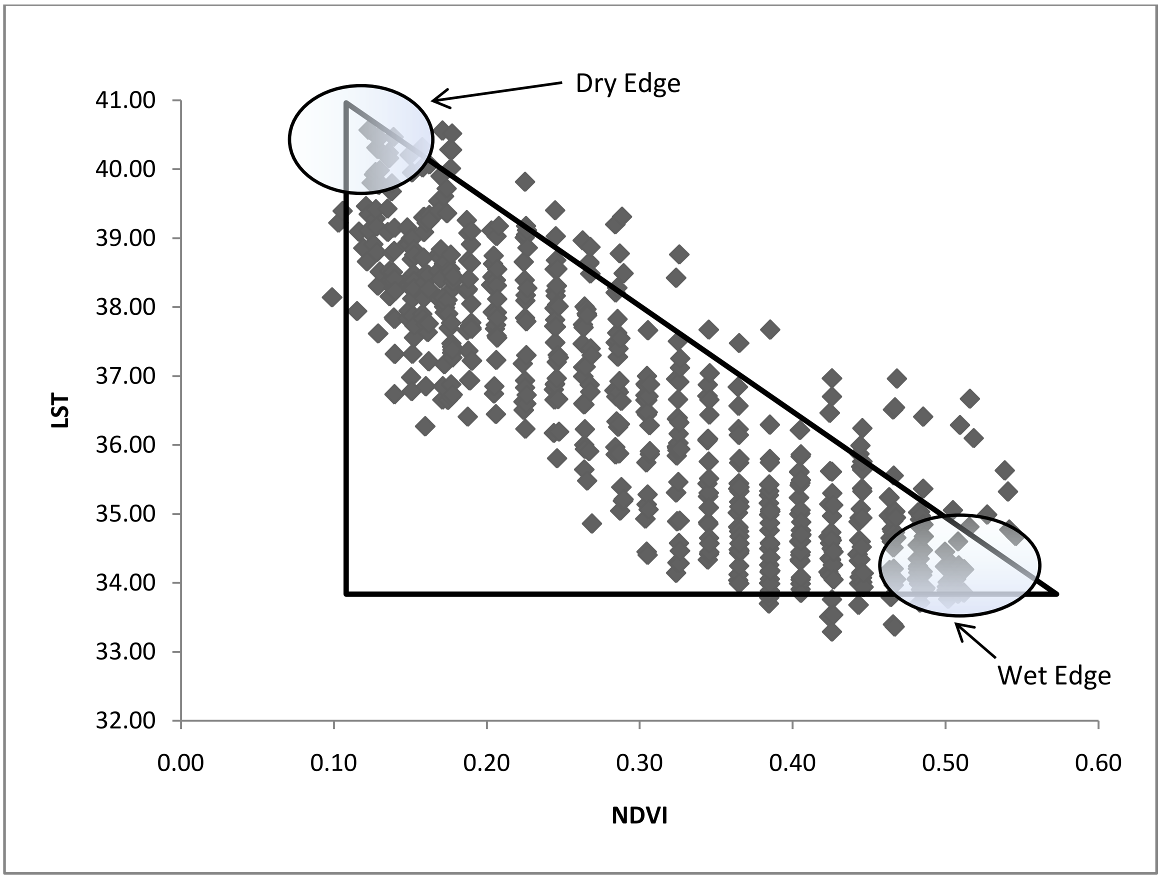

Figure 12. Land surface temperature and normalized difference vegetation index distribution of sample points using scatter plot.

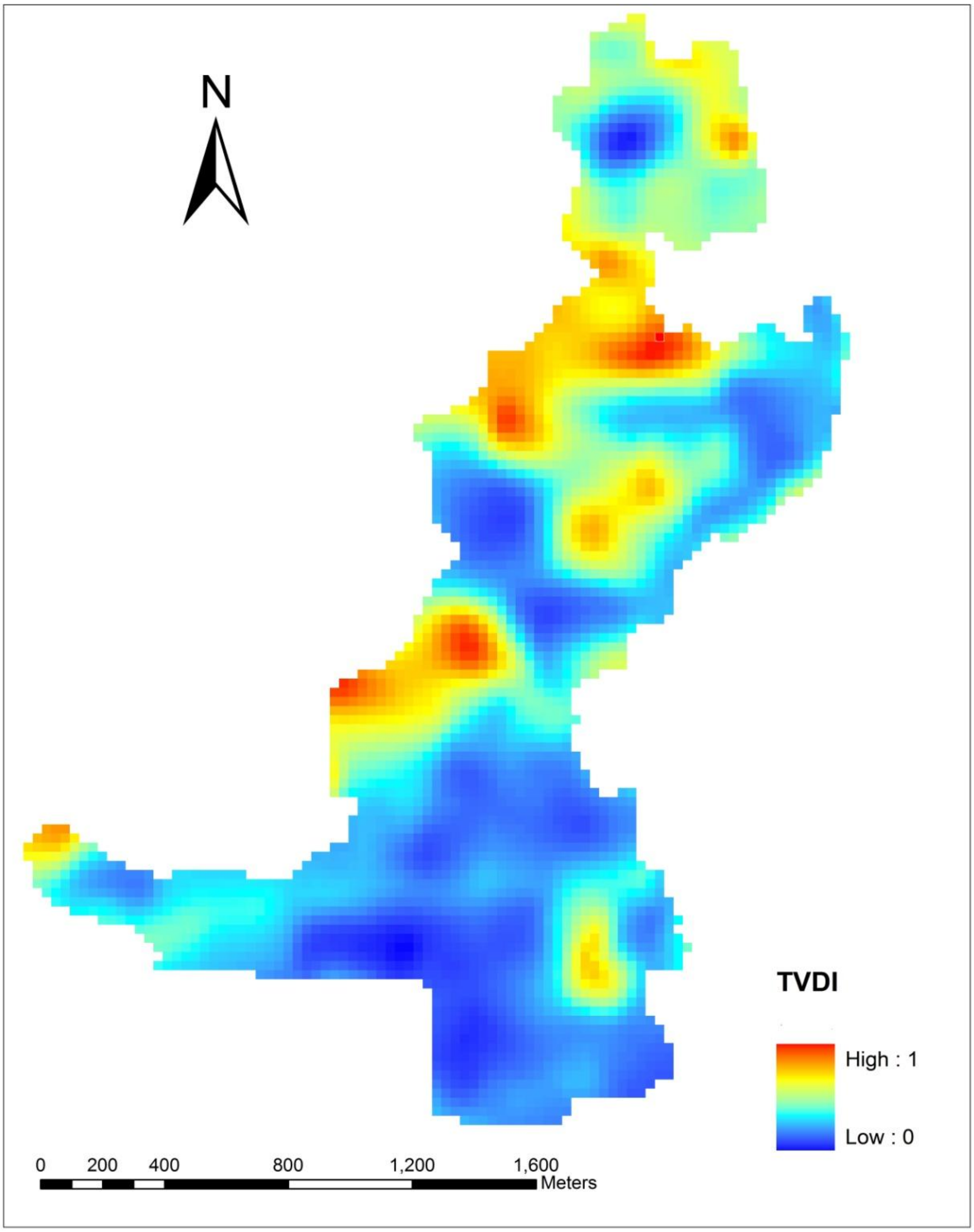

Figure 13. Temperature vegetation dryness index surface of study area.

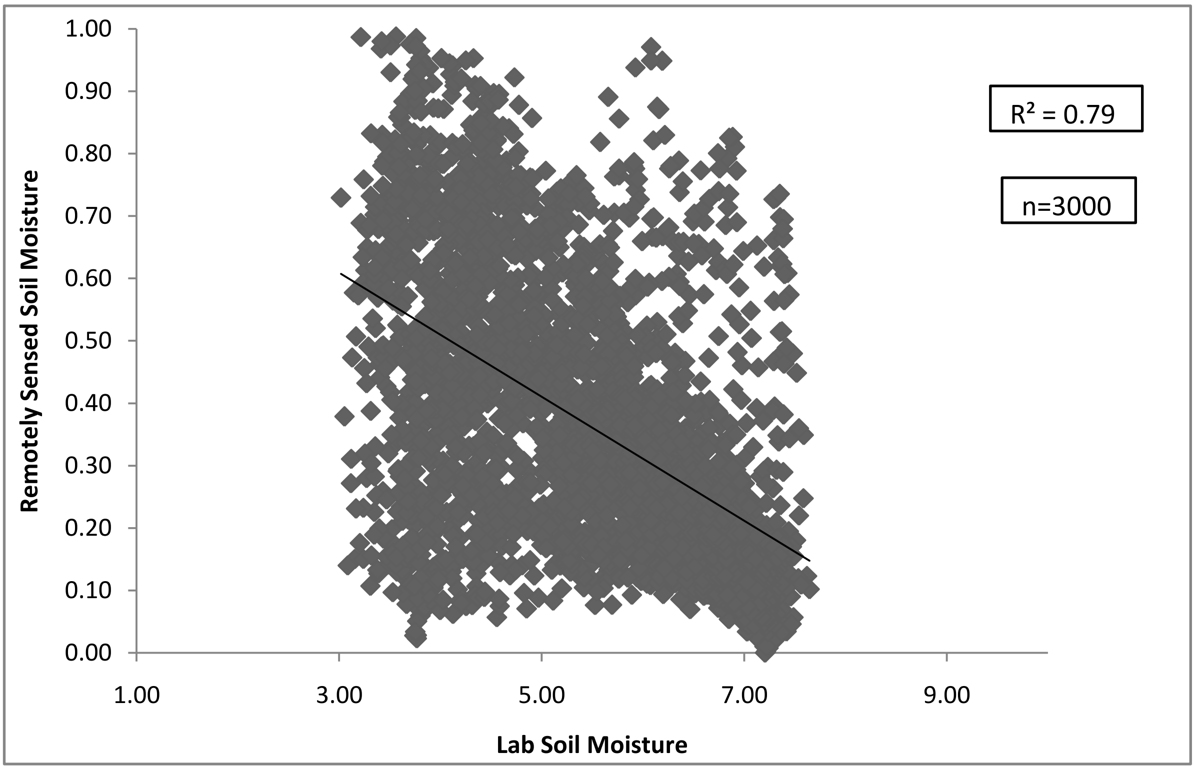

Figure 14. Correlation between remotely sensed soil moisture and lab soil moisture.

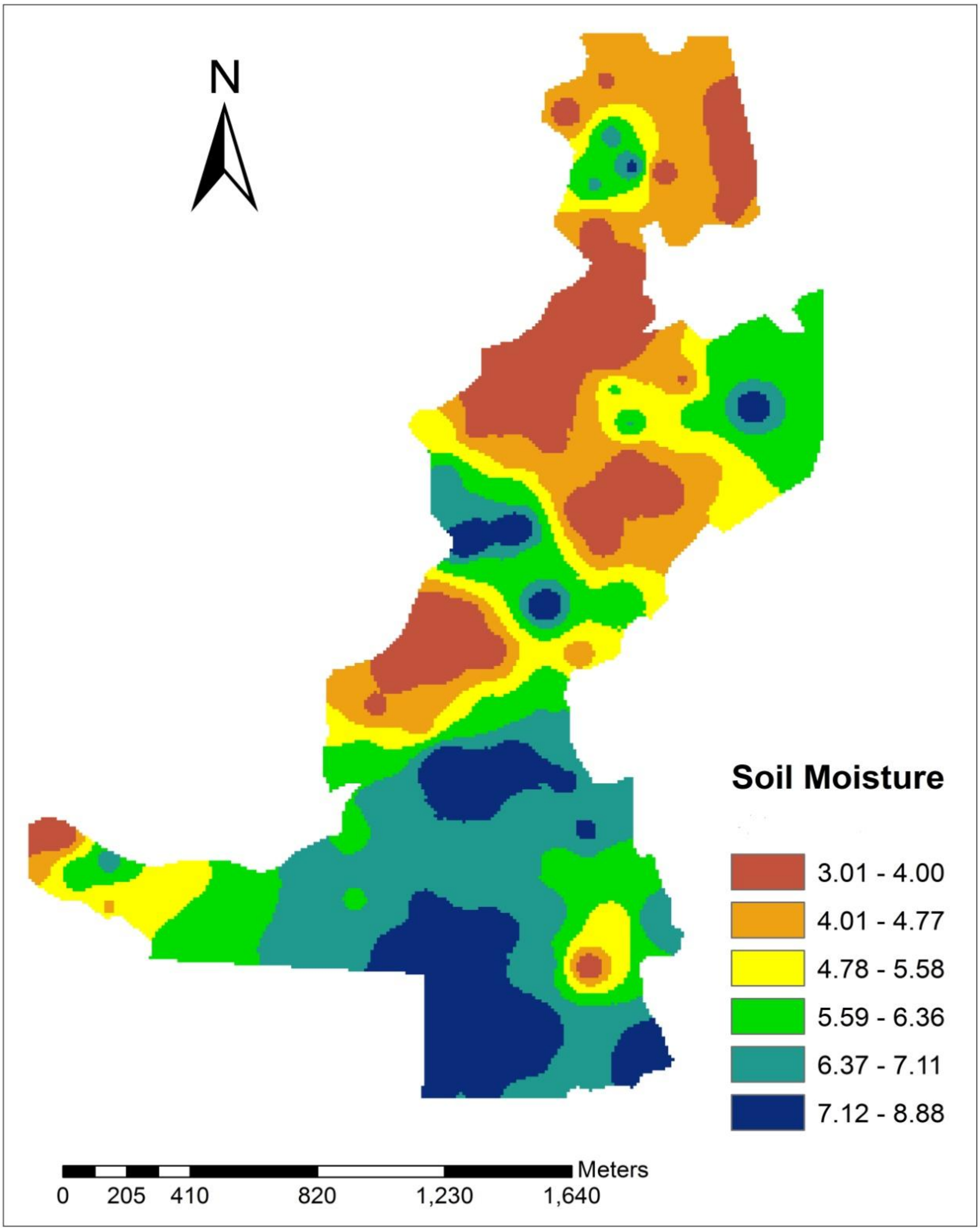

Figure 15. Final soil moisture map of study area.

Chapter 4

CONCLUSIONS AND RECOMMENDATIONS

The study examined different methods for estimation of surface soil moisture. In situ measurements were taken from study area located at NARC Islamabad. The samples were analyzed for moisture determination by using traditional method. FTIR analysis was carried out to study the effect of reflectance on different moisture conditions. A general trend was found that as the soil moisture increases reflectance decreases and vice versa. The FTIR analysis should be more precise as repeated measurements should be taken by applying different type of soils under various moisture conditions. This will form standard criteria to estimate soil moisture directly by using FTIR spectroscopy. The third method was remotely sensed soil moisture estimation. Landsat 8 imagery of the study area was used for estimation. Triangulation method was applied which found good for appropriate estimation of soil moisture. Strong correlation was found between LST & NDVI which results in the formation of TVDI surface by using regression analysis. TVDI surface was then correlated with in situ soil measurements. The results shown moderately strong correlation which means that almost 60 percent results were satisfactory. So from above study it is concluded that remotely sensed data can be used for the estimation of surface soil moisture as it is less time and resource consuming. It can be applied on large scale. Regular monitoring of soil moisture can be made for agriculture management, drought management, decision making. It can also be used in hydrological modeling where soil moisture is a key component.

REFERENCES

Akkuzu, E., Kaya, U., Camoglu, G., Mengu, G. P., & Asik, S. (2013). Determination of Crop Water Stress Index and Irrigation Timing on Olive Trees Using a Handheld Infrared Thermometer. *Journal of Irrigation and Drainage Engineering, 139*(9), 728-737.

Al-Jassar, H. K., & Rao, K. S. (2010). Monitoring of soil moisture over the Kuwait desert using remote sensing techniques. *International Journal of Remote Sensing, 31*(16), 4373-4385.

Albergel, C., Dorigo, W., Reichle, R. H., Balsamo, G., de Rosnay, P., Munoz-Sabater, J., et al. (2013). Skill and Global Trend Analysis of Soil Moisture from Reanalyses and Microwave Remote Sensing. *Journal of Hydrometeorology, 14*(4), 1259-1277.

Albergel, C., Rudiger, C., Calvet, J. C., Carrer, D., Fritz, N. E. D., & Pellarin, T. (2010). Use of in-situ soil moisture measurements to evaluate microwave remote sensing products in south-western France. *Houille Blanche-Revue Internationale De L Eau*(2), 120-126.

Atchley, A. L., & Maxwell, R. M. (2011). Influences of subsurface heterogeneity and vegetation cover on soil moisture, surface temperature and evapotranspiration at hillslope scales. *Hydrogeology Journal, 19*(2), 289-305.

Benedetto, A., & Benedetto, F. (2011). Remote Sensing of Soil Moisture Content by GPR Signal Processing in the Frequency Domain. *Ieee Sensors Journal, 11*(10), 2432-2441.

Bezerra, B. G., dos Santos, C. A. C., da Silva, B. B., Perez-Marin, A. M., Bezerra, M. V. C., Bezerra, J. R. C., et al. (2013). Estimation of Soil Moisture in the Root-Zone from Remote Sensing Data. *Revista Brasileira De Ciencia Do Solo, 37*(3), 596-603.

Blumberg, D., Freilikher, V., Kaganovskii, Y., & Maradudin, A. (2002). Subsurface microwave remote sensing of soil-water content: field studies in the Negev Desert and optical modelling. *International Journal of Remote Sensing, 23*(19), 4039-4054.

Bowers, S., & Hanks, R. (1965). Reflection of radiant energy from soils. *Soil Science, 100*(2), 130-138.

Brosinsky, A., Lausch, A., Doktor, D., Salbach, C., Merbach, I., Gwillym-Margianto, S., et al. (2014). Analysis of Spectral Vegetation Signal Characteristics as a Function of Soil Moisture Conditions Using

Hyperspectral Remote Sensing. *Journal of the Indian Society of Remote Sensing*, *42*(2), 311-324.

Campbell, J. (2009). Remote sensing of soils. *The SAGE Handbook of Remote Sensing, 1*.

Carlson, T. (2007). An overview of the" triangle method" for estimating surface evapotranspiration and soil moisture from satellite imagery. *Sensors, 7*(8), 1612-1629.

Carlson, T. N., Gillies, R. R., & Schmugge, T. J. (1995). An interpretation of methodologies for indirect measurement of soil water content. *Agricultural and Forest Meteorology, 77*(3), 191-205.

Chauhan, N., Miller, S., & Ardanuy, P. (2003). Spaceborne soil moisture estimation at high resolution: a microwave-optical/IR synergistic approach. *International Journal of Remote Sensing, 24*(22), 4599-4622.

Choi, M., Kim, T. W., & Kustas, W. P. (2011). Reliable estimation of evapotranspiration on agricultural fields predicted by the Priestley-Taylor model using soil moisture data from ground and remote sensing observations compared with the Common Land Model. *International Journal of Remote Sensing, 32*(16), 4571-4587.

Cohen M.J., P. J. P., DeBusk W.F. (2005). Visible-near infrared reflectance spectroscopy for rapid, non-destructive assessment of wetland soil quality. *Journal of Environmental Quality*, *34*, 1422–1434.

dall'Amico, J. T., Schlenz, F., Loew, A., Mauser, W., Kainulainen, J., Balling, J. E., et al. (2013). The SMOS Validation Campaign 2010 in the Upper Danube Catchment: A Data Set for Studies of Soil Moisture, Brightness Temperature, and Their Spatial Variability Over a Heterogeneous Land Surface. *Ieee Transactions on Geoscience and Remote Sensing, 51*(1), 364-377.

Engman, E. a. C., N. (1995). Status of microwave soil moisture measurements with remote sensing. *Remote Sensing of Environment*, *51*, 189-198.

Engman, E. T. (1991). Applications of Microwave Remote-Sensing of Soil-Moisture for Water-Resources and Agriculture. *Remote Sensing of Environment*, *35*(2-3), 213-226.

Fan, Y., & van den Dool, H. (2011). Bias Correction and Forecast Skill of NCEP GFS Ensemble Week-1 and Week-2 Precipitation, 2-m Surface Air Temperature, and Soil Moisture Forecasts. *Weather and Forecasting, 26*(3), 355-370.

Fang, B., Lakshmi, V., Bindlish, R., Jackson, T. J., Cosh, M., & Basara, J. (2013a). Passive Microwave Soil Moisture Downscaling Using Vegetation Index and Skin Surface Temperature. *Vadose Zone Journal, 12*(3).

Fang, B., Lakshmi, V., Bindlish, R., Jackson, T. J., Cosh, M., & Basara, J. (2013b). Passive Microwave Soil Moisture Downscaling Using Vegetation Index and Skin Surface Temperature (vol 12, 0089, 2013). *Vadose Zone Journal, 12*(4).

Gao, S. G., Zhu, Z. L., Liu, S. M., Jin, R., Yang, G. C., & Tan, L. (2014). Estimating the spatial distribution of soil moisture based on Bayesian maximum entropy method with auxiliary data from remote sensing. *International Journal of Applied Earth Observation and Geoinformation, 32*, 54-66.

Goetz, S. J., Prince, S. D., & Small, J. (2000). Advances in satellite remote sensing of environmental variables for epidemiological applications. *Adv Parasitol, 47*, 289-307.

Goward, S. N., Xue, Y., & Czajkowski, K. P. (2002). Evaluating land surface moisture conditions from the remotely sensed temperature/vegetation index measurements: an exploration with the simplified simple biosphere model. *Remote Sensing of Environment, 79*(2), 225-242.

Gruhier, C., De Rosnay, P., Kerr, Y., Mougin, E., Ceschia, E., Calvet, J. C., et al. (2008). Evaluation of AMSR-E soil moisture product based on ground measurements over temperate and semi-arid regions. *Geophysical Research Letters, 35*(10).

Guo, D. L., Yang, M. X., & Wang, H. J. (2011). Sensible and latent heat flux response to diurnal variation in soil surface temperature and moisture under different freeze/thaw soil conditions in the seasonal frozen soil region of the central Tibetan Plateau. *Environmental Earth Sciences, 63*(1), 97-107.

Haberhauer, G., & Gerzabek, M. (1999). Drift and transmission FT-IR spectroscopy of forest soils: an approach to determine decomposition processes of forest litter. *Vibrational Spectroscopy, 19*(2), 413-417.

Hassan, Q. K., Bourque, C. P.-A., Meng, F.-R., & Cox, R. M. (2007). A wetness index using terrain-corrected surface temperature and normalized difference vegetation index derived from standard MODIS products: An evaluation of its use in a humid forest-dominated region of eastern Canada. *Sensors, 7*(10), 2028-2048.

Hejazi, A., & Woodbury, A. D. (2011). Evaluation of Land Surface Scheme SABAE-HW in Simulating Snow Depth, Soil Temperature and Soil

Moisture within the BOREAS Site, Saskatchewan. *Atmosphere-Ocean, 49*(4), 408-420.

Holzman, M. E., Rivas, R., & Piccolo, M. C. (2014). Estimating soil moisture and the relationship with crop yield using surface temperature and vegetation index. *International Journal of Applied Earth Observation and Geoinformation, 28*, 181-192.

Kerr, Y. H., Waldteufel, P., Wigneron, J.-P., Martinuzzi, J., Font, J., & Berger, M. (2001). Soil moisture retrieval from space: The Soil Moisture and Ocean Salinity (SMOS) mission. *Geoscience and Remote Sensing, IEEE Transactions on, 39*(8), 1729-1735.

Liu, F., Liu, C. Q., Wang, S. L., & Zhu, Z. J. (2012). Soil temperature and moisture controls on surface fluxes and profile concentrations of greenhouse gases in karst area in central part of Guizhou Province, southwest China. *Environmental Earth Sciences, 67*(5), 1431-1439.

Lobell, D. B., & Asner, G. P. (2002). Moisture effects on soil reflectance. *Soil Science Society of America Journal, 66*(3), 722-727.

Lopes, H. L., Accioly, L. J. D., da Silva, F. H. B. B., Sobral, M. D. M., de Araujo, J. C., & Candeias, A. L. B. (2011). Spatial distribution of soil moisture using land surface temperature and vegetation indices. *Revista Brasileira De Engenharia Agricola E Ambiental, 15*(9), 973-980.

Mei, R., & Wang, G. L. (2011). Impact of Sea Surface Temperature and Soil Moisture on Summer Precipitation in the United States Based on Observational Data. *Journal of Hydrometeorology, 12*(5), 1086-1099.

Moran, M., Clarke, T., Inoue, Y., & Vidal, A. (1994). Estimating crop water deficit using the relation between surface-air temperature and spectral vegetation index. *Remote Sensing of Environment, 49*(3), 246-263.

Mouazen, A. M., Karoui, R., De Baerdemaeker, J., & Ramon, H. (2006). Characterization of soil water content using measured visible and near infrared spectra. *Soil Science Society of America Journal, 70*(4), 1295-1302.

Muller, E., & Decamps, H. (2001). Modeling soil moisture–reflectance. *Remote Sensing of Environment, 76*(2), 173-180.

Naira, C., Robert, L., Ramata, M., & Marouane, T. (2007). *Surface soil moisture status over the Mackenzie River Basin using a temperature/vegetation index.* Paper presented at the Geoscience and Remote Sensing Symposium, 2007. IGARSS 2007. IEEE International.

Nemani, R., Pierce, L., Running, S. and Goward, S. (1992). Developing satellite derived estimates of surface moisture status. *Journal of Applied Meteorology, 32,* 548-557.

Parinussa, R. M., Holmes, T. R. H., Yilmaz, M. T., & Crow, W. T. (2011). The impact of land surface temperature on soil moisture anomaly detection from passive microwave observations. *Hydrology and Earth System Sciences, 15*(10), 3135-3151.

Patel, N., Anapashsha, R., Kumar, S., Saha, S., & Dadhwal, V. (2009). Assessing potential of MODIS derived temperature/vegetation condition index (TVDI) to infer soil moisture status. *International Journal of Remote Sensing, 30*(1), 23-39.

Patterson, T. (2013). Landsat 8 Photoshop Tutorial.

Pause, M., Schulz, K., Zacharias, S., & Lausch, A. (2012). Near-surface soil moisture estimation by combining airborne L-band brightness temperature observations and imaging hyperspectral data at the field scale. *Journal of Applied Remote Sensing, 6*.

Pollacco, J. A. P., & Mohanty, B. P. (2012). Uncertainties of Water Fluxes in Soil-Vegetation-Atmosphere Transfer Models: Inverting Surface Soil Moisture and Evapotranspiration Retrieved from Remote Sensing. *Vadose Zone Journal, 11*(3).

Pratt, D., & Ellyett, C. (1979). The thermal inertia approach to mapping of soil moisture and geology. *Remote Sensing of Environment, 8*(2), 151-168.

Price, J. (1990.). Using spatial context in satellite data to infer regional scale evapotranspiration. *IEEE Transactions on Geoscience and Remote Sensing 28,* 940-948.

Ridler, M. E., Sandholt, I., Butts, M., Lerer, S., Mougin, E., Timouk, F., et al. (2012). Calibrating a soil-vegetation-atmosphere transfer model with remote sensing estimates of surface temperature and soil surface moisture in a semi arid environment. *Journal of Hydrology, 436,* 1-12.

Ryan, J., Estefan, G., & Rashid, A. (2007). *Soil and plant analysis laboratory manual*: ICARDA.

Sandholt, I., Rasmussen, K., & Andersen, J. (2002). A simple interpretation of the surface temperature/vegetation index space for assessment of surface moisture status. *Remote Sensing of Environment, 79*(2), 213-224.

Song, C. Y., Jia, L., & Menenti, M. (2014). Retrieving High-Resolution Surface Soil Moisture by Downscaling AMSR-E Brightness Temperature Using

MODIS LST and NDVI Data. *Ieee Journal of Selected Topics in Applied Earth Observations and Remote Sensing, 7*(3), 935-942.

Song, X. N., Leng, P., Li, X. T., Li, X. H., & Ma, J. W. (2013). Retrieval of daily evolution of soil moisture from satellite-derived land surface temperature and net surface shortwave radiation. *International Journal of Remote Sensing, 34*(9-10), 3289-3298.

Srivastava, P. K., Han, D. W., Ramirez, M. R., & Islam, T. (2013). Machine Learning Techniques for Downscaling SMOS Satellite Soil Moisture Using MODIS Land Surface Temperature for Hydrological Application. *Water Resources Management, 27*(8), 3127-3144.

Stenberg, B., Viscarra Rossel, R. A., Mouazen, A. M., & Wetterlind, J. (2010). Chapter Five-Visible and Near Infrared Spectroscopy in Soil Science. *Advances in agronomy, 107*, 163-215.

Sun, L., Sun, R., Li, X. W., Liang, S. L., & Zhang, R. H. (2012). Monitoring surface soil moisture status based on remotely sensed surface temperature and vegetation index information. *Agricultural and Forest Meteorology, 166*, 175-187.

Tennant, W., & Beare, S. (2014). New schemes to perturb sea-surface temperature and soil moisture content in MOGREPS. *Quarterly Journal of the Royal Meteorological Society, 140*(681), 1150-1160.

Verstraeten, W. W., Veroustraete, F., & Feyen, J. (2005). Soil moisture retrieval from optical and thermal spaceborne remote sensing. *Commun Agric Appl Biol Sci, 70*(2), 27-30.

Verstraeten, W. W., Veroustraete, F., van der Sande, C. J., Grootaers, I., & Feyen, J. (2006). Soil moisture retrieval using thermal inertia, determined with visible and thermal spaceborne data, validated for European forests. *Remote Sensing of Environment, 101*(3), 299-314.

Vinnikov, K. Y., Robock, A., Qiu, S., Entin, J. K., Owe, M., Choudhury, B. J., et al. (1999). Satellite remote sensing of soil moisture in Illinois, United States. *Journal of Geophysical Research: Atmospheres (1984–2012), 104*(D4), 4145-4168.

Viscarra Rossel, R., & McBratney, A. (1998). Laboratory evaluation of a proximal sensing technique for simultaneous measurement of soil clay and water content. *Geoderma, 85*(1), 19-39.

Walker, J. P., Willgoose, G. R., & Kalma, J. D. (2004). In situ measurement of soil moisture: a comparison of techniques. *Journal of Hydrology, 293*(1), 85-99.

Wang, A. Q., Xie, C., Shi, J. C., & Gong, H. L. (2013). The Relationship Between the Variation Rate of MODIS Land Surface Temperature and AMSR-E Soil Moisture and Its Application to Downscaling. *Spectroscopy and Spectral Analysis, 33*(3), 623-627.

Wang, L., & Qu, J. J. (2009). Satellite remote sensing applications for surface soil moisture monitoring: a review. *Frontiers of Earth Science in China, 3*(2), 237-247.

Wang, W., Huang, D., Wang, X. G., Liu, Y. R., & Zhou, F. (2011). Estimation of soil moisture using trapezoidal relationship between remotely sensed land surface temperature and vegetation index. *Hydrology and Earth System Sciences, 15*(5), 1699-1712.

Wu, S. H., Jansson, P. E., & Zhang, X. Y. (2011). Modelling temperature, moisture and surface heat balance in bare soil under seasonal frost conditions in China. *European Journal of Soil Science, 62*(6), 780-796.

Zeng, Y., Feng, Z. and Xiang, N. (2004). *Assessment of soil moisture using Landsat ETM+ temperature/vegetation index in semiarid environment.* Paper presented at the Proceedings of the IEEE International Geoscience and Remote Sensing Symposium.

Zhao, W., & Li, Z. L. (2013). Sensitivity study of soil moisture on the temporal evolution of surface temperature over bare surfaces. *International Journal of Remote Sensing, 34*(9-10), 3314-3331.

Zhao, W., Li, Z. L., Wu, H., Tang, B. H., Zhang, X. Y., Song, X. N., et al. (2013). Determination of bare surface soil moisture from combined temporal evolution of land surface temperature and net surface shortwave radiation. *Hydrological Processes, 27*(19), 2825-2833.

APPENDICES

Appendix-1. Raw soil moisture data along with the geographic coordinates collected from the study area.

X-Coordinate	Y-Coordinate	Soil Moisture
326543.47	3728802.08	4.10
326505.56	3728650.46	3.90
326700.51	3728655.87	4.20
326835.89	3728726.27	4.10
326386.42	3728542.15	3.60
326521.80	3728471.75	6.70
326738.41	3728504.25	4.50
326895.46	3728542.15	3.20
326927.95	3728395.94	3.50
326684.26	3728352.62	3.40
326467.65	3728309.30	6.50
326473.07	3728163.08	3.60
326895.46	3728233.48	3.90
326565.13	3728022.29	3.40
326733.00	3728157.67	4.40
326418.91	3727930.23	3.90
326586.79	3727865.25	3.20
326348.52	3727805.68	3.50
326521.80	3727746.11	3.10
326588.95	3728370.13	7.40
326230.27	3727730.60	3.20
326351.35	3727673.48	3.60
326132.03	3727627.79	3.20
325967.54	3727488.43	5.40
326081.77	3727506.71	3.70
326186.86	3727566.11	3.00
326351.35	3727570.68	3.80
326531.83	3727630.08	5.70
326582.09	3727518.13	6.40
326326.22	3727461.02	3.80
326202.85	3727401.62	4.50
325985.82	3727339.94	6.90
326013.24	3727241.70	6.40
325729.95	3726430.68	5.80
325791.63	3726270.76	6.80

325981.25	3726384.99	8.70
325937.85	3726190.80	7.10
325686.54	3726167.96	5.90
325791.63	3726083.43	6.60
325912.72	3725934.93	7.20
325557.37	3726065.15	6.80
325696.73	3725941.79	6.20
325838.37	3725770.44	7.50
325664.75	3725759.02	7.10
325545.95	3725907.52	6.80
325465.99	3725786.44	6.50
325335.77	3725973.77	5.80
325169.00	3726021.75	5.30
326196.00	3727291.96	6.20
326376.48	3727346.79	4.00
326582.09	3727394.77	3.50
326753.43	3727664.34	3.90
326789.99	3727552.40	6.00
326885.94	3727710.04	6.30
326988.74	3727744.30	5.60
327139.52	3727771.72	5.90
327201.21	3727890.52	6.30
327196.64	3727632.36	5.80
327155.52	3727467.87	6.10
326977.32	3727575.25	8.10
327057.28	3727349.07	5.60
326824.25	3727369.64	4.50
326687.18	3727298.81	3.00
326892.79	3727205.15	4.90
326678.04	3727113.77	4.70
326492.99	3727129.76	3.40
326426.74	3727225.71	3.10
326216.56	3727173.16	8.50
326061.21	3727134.33	8.90
326266.82	3727061.22	5.90
326106.90	3727029.24	5.60
326554.68	3726944.71	6.10
326307.94	3726917.29	8.20

325949.27	3726908.15	3.20
326049.79	3726880.74	3.00
326132.03	3726764.23	3.30
325978.97	3726727.67	3.40
325839.61	3726691.12	3.60
325764.22	3726576.89	3.80
325903.58	3726533.49	4.20
326125.18	3726579.18	5.80
326413.03	3726755.09	4.30
326192.48	3726024.03	6.40
326363.82	3726060.58	5.90
326537.45	3726035.45	5.60
326674.52	3725880.10	7.10
326311.28	3725896.09	6.90
326167.35	3725838.98	7.70
326299.85	3725731.61	6.80
326059.97	3725576.26	7.40
325948.03	3725512.29	7.60
326034.84	3725292.97	7.10
326240.45	3725295.26	6.80
326162.78	3725441.47	8.30
326274.72	3725528.28	8.00
326416.37	3725377.50	6.60